ARTICLE
Journal of Cellular Biochemistry 111:1482–1492 (2010)

Journal of Cellular Biochemistry

Screening and Identification of Differentially Expressed Genes in Goose Hepatocytes Exposed to Free Fatty Acid

Zhixiong Pan,[1] Jiwen Wang,[1*] Bo Kang,[1] Lizhi Lu,[2] Chunchun Han,[1] Hui Tang,[1] Liang Li,[1] Feng Xu,[1] Zehui Zhou,[1] and Jia LV[1]

[1]*Key Laboratory of Animal Genetic Resources, College of Animal Science and Technology, Sichuan Agricultural University, Ya'an, Sichuan 625014, P.R. China*

[2]*Institute of Animal Science and Veterinary Medicine, Zhejiang Academy of Agricultural Science, Hangzhou, Zhejiang 310021, P.R. China*

ABSTRACT

The overaccumulation of triglycerides in hepatocytes induces hepatic steatosis; however, little is known about the mechanism of goose hepatic steatosis. The aim of this study was to define an experimental model of hepatocellular steatosis with TG overaccumulation and minimal cytotoxicity, using a mixture of various proportions of oleate and palmitate free fatty acids (FFAs) to induce fat-overloading, then using suppressive subtractive hybridization and a quantitative PCR approach to identify genes with higher or lower expression levels after the treatment of cells with FFA mixtures. Overall, 502 differentially expressed clones, representing 21 novel genes and 87 known genes, were detected by SSH. Based on functional clustering, up- and down-regulated genes were mostly related to carbohydrate and lipid metabolism, enzyme activity and signal transduction. The expression of 20 selected clones involved with carbohydrate and lipid metabolism pathways was further studied by quantitative PCR. The data indicated that six clones similar to the genes ChREBP, FoxO1, apoB, IHPK2, KIF1B, and FSP27, which participate in de novo synthesis of fatty acid and secretion of very low density lipoproteins, had significantly lower expression levels in the hepatocytes treated with FFA mixtures. Meanwhile, 13 clones similar to the genes DGAT-1, ACSL1, DHRS7, PPARα, L-FABP, DGAT-2, PCK, ACSL3, CPT-1, A-FABP, PPARβ, MAT, and ALDOB had significantly higher expression levels in the hepatocytes treated with FFA mixtures. These results suggest that several metabolic pathways are altered in goose hepatocytes, which may be useful for further research into the molecular mechanism of goose hepatic steatosis. J. Cell. Biochem. 111: 1482–1492, 2010.

KEY WORDS: HEPATIC STEATOSIS; GENE EXPRESSION; SUPPRESSIVE SUBTRACTIVE HYBRIDIZATION; OLEIC ACID; PALMITIC ACID; GOOSE

Hepatic steatosis refers to the condition of overaccumulation of triglycerides (TG) in hepatocytes. In mammals, TG accumulation in the liver by sustained alcohol intake, obesity, and metabolic or infectious disease, was thought to be an inert histological epiphenomenon and is associated with several metabolic diseases [den Boer et al., 2004; Dowman et al., 2010]. However, under natural conditions, birds, especially some wild waterfowl, exhibit non-pathological hepatic steatosis as a result of energy storage before migration [Fournier et al., 1997; Pilo and George, 1983]. This specific capability is used for the production of commercial fatty liver in waterfowl production. Fong et al. [Fong et al., 2000] and Fournier et al [Fournier et al., 1997] reported that the accumulation of TG within hepatocytes was caused by a disturbed equilibrium between liver TG synthesis and secretion, dietary intake or endogenous synthesis could lead to accumulation of TG in the hepatocytes when mitochondrial β-oxidation and very low density lipoprotein-TG (VLDL-TG) secretion and production were not capable of processing all incoming free acid [Bradbury, 2006; Hermier et al., 1988]. When fat accumulates, lipids are primarily stored in the cytoplasm as TG. However, the goose genome has not been thoroughly studied, and little information is available concerning the genes involved in maintaining metabolic homeostasis in conditions of TG overaccumulation in birds.

Discerning universal mechanisms of metabolic pathways can be difficult in animal models with either individual or environmental differences. In mammals, hepatocytes that were induced by fat-overloading to develop of hepatic steatosis with oleate or palmitate are broadly discussed, and different free fatty acids (FFAs) have distinct

*Correspondence to: Prof. Jiwen Wang, College of Animal Science and Technology, Sichuan Agricultural University, Ya'an, Sichuan 625014, P.R. China. E-mail: wjw2886166@163.com

Received 23 March 2010; Accepted 1 September 2010 • DOI 10.1002/jcb.22878 • © 2010 Wiley-Liss, Inc.
Published online 24 September 2010 in Wiley Online Library (wileyonlinelibrary.com).

influences depending upon the cell type [Miller et al., 2005; Donato et al., 2006; Malhi et al., 2006]. Gomez-Lechon et al. indicate that an FFA mixture (oleate/palmitate at a 2:1 ratio) is associated with minor toxic and apoptotic effects, the FFA mixture suitable to experimentally investigate the impact of fat overaccumulation in the hepatocytes [Gomez-Lechon et al., 2007]. In addition, oleate (C18:1) and palmitate (C16:0) are the most abundant fatty acids in the diet and in the goose fatty liver [Molette et al., 2001]. SSH is a highly efficient and widely used polymerase chain reaction (PCR)-based method for identifying differentially expressed genes [Thais Martins de Lima et al., 2004; Diatchenko et al., 1996]. Therefore, the primary hepatocytes of Sichuan White geese were incubated with mixtures containing various proportions of saturated (palmitate) and unsaturated (oleate) FFAs to induce the accumulation of TG and were subjected to the SSH and real-time PCR techniques to isolate genes with expression regulated by oleic acid and palmitic acid treatment. In SSH, differentially expressed sequences were enriched, and the concentration of high- and low-abundance sequences was equalized. The identification of differentially expressed genes is an initial step in exploring the molecular mechanisms of hepatic steatosis in birds.

MATERIALS AND METHODS

PRIMARY HEPATOCYTE ISOLATION AND CULTURE

Hepatocytes were isolated from six 30-day-old Sichuan white geese (Anser cygnoides), which were hatched on the same day and grown under natural conditions of light and temperature at the Experimental Farm for Waterfowl Breeding at Sichuan Agricultural University by a modified method described by Seglen [Seglen, 1976]. Cell viability was assessed by the Trypan blue dye exclusion test. Freshly isolated hepatocytes were diluted to 1×10^6 cells/mL. Culture medium was composed of DMEM (containing 4.5 g/L glucose; GIBCO, USA) with 100 IU/L insulin (Sigma, USA), 100 IU/mL penicillin (Sigma, USA), 100 g/mL streptomycin (Sigma, USA), 2 mmol/L glutamine (Sigma, USA), and 100 mL/L fetal bovine serum (Clark, Australia). The hepatocytes were then plated in 24-well plates and 96-well plates for measurement of TG level and cell viability, which were used to select suitable proportion of oleate and palmitate for further experiment. Next, hepatocytes were plated in 60-mm culture dishes at 3×10^6 cells per dish for the preparation of total RNA for SSH and real-time quantitative PCR. Cultures were incubated at 40% in a humidified atmosphere containing 5% CO_2 with medium replaced after 3 h, followed by serum-free media replacement after 24 h.

FAT-OVERLOADING INDUCTION IN HEPATOCYTES

To induce fat-overloading of cells, primary cultures of goose hepatocytes were exposed to a long-chain mixture of FFAs (oleate and palmitate) at various ratios. Stock solutions of 50 mM oleate acid and 50 mM palmitate, prepared in culture medium containing 1% bovine serum albumin, were conveniently diluted in culture medium to obtain the desired final concentrations [Gomez-Lechon et al., 2007]. The FFA mixtures were added to hepatocytes 24 after seeding.

MEASUREMENT OF TG ACCUMULATION

Samples of cultured cells for each treatment were shaken for 1 h using an ultrasonic processor, then washed three times with ice-cold phosphate-buffered saline and added to an isovolumic mixture of chloroform and methanol (2:1 v/v). The TG level was quantified by a colorimetric enzymatic method [Fossati and Prencipe, 1982] using a Triglyceride GPO-POD assay kit (Biosino, Beijing, China).

MTT ASSAY

The assay for cell viability was performed according to Francesco et al. [Natali et al., 2007], with some modifications. Primary cultures of goose hepatocytes were plated at a density of 0.5×10^4 cells/well in a 96-well culture dish. After 24 h, the serum-rich medium was refreshed, and cells were incubated for 24 h with the indicated fatty acid sodium salts. Next, cell monolayers were incubated for 4 h with 1 mg/mL MTT. Mitochondria of living cells can convert the yellow tetrazolium compound to its purple formazan derivative. After removal of the unconverted MTT, the formazan product was dissolved in isopropanol, and the absorbance of formazan dye was measured at 570 nm. Viability was calculated as percentage of absorbance relative to control cells.

CASPASE-3 ACTIVITY

Measurement of caspase-3 activity was achieved using a kit (BESTBIO, Beijing, China), according to the manufacturer's instructions. After the hepatocytes were incubated for increasing periods of time with the different treatments, detached cells were collected by centrifugation at 500*g* for 3 min, and attached cells were scraped off. Caspases-3 activity was measured using the specific fluorogenic substrates 10 μL Ac-DEVD-AMC, as previously described in detail [Gomez-Lechon et al., 2003].

CONSTRUCTION OF SUBTRACTED cDNA LIBRARIES BY SSH

Total RNA of both control hepatocytes and hepatocytes treated with FFA mixtures (oleate/palmitate) at a 2:1 ratio was extracted using a TRIzol Reagent (Invitrogen Corporation). The quality of the total sample was vital to the successful construction of the SSH cDNA libraries. Thus, total RNA quantification and integrity were strictly examined by spectrophotometry and 1.0% agarose electrophoresis. Poly(A)$^+$ RNA was prepared from total RNA using an Oligotex mRNA minikit (Qiagen). SSH [Diatchenko et al., 1996] was performed by using a PCR-select cDNA subtraction kit (Clontech), according to the manufacturer's instructions. Two reciprocally subtracted cDNA libraries were generated using 4 μg of each of the two mRNA populations described above to synthesize the corresponding double stranded cDNAs. Briefly, by using the cDNA synthesized from the primary hepatocytes treated with FFAs as the "tester" and the cDNA from the primary hepatocytes of the control as the "driver" (see the Clontech subtraction kit user manual), SSH-1 was constructed. We expected this library to be enriched in partial transcripts of genes upregulated in hepatocytes treated with the FFA mixture. The reciprocal library, corresponding to genes down-regulated in hepatocytes treated with FFA mixtures (SSH-2), was constructed by using the cDNA from the control as the "tester" and the cDNA from the hepatocytes treated with FFA as the "driver". After PCR amplification, subtracted products were cloned into a pGEM-T Easy vector (Promega) and introduced into Escherichia coli XL1-Blue competent cells. Plated bacteria were grown overnight, recovered in 150 μL of LB medium per plate and frozen at −80%

after adding 15% glycerol. From each library, 100 μL of a 10^{-5} dilution was plated, and 600 (corresponding to six 96-well plates) white recombinant colonies were picked from each library.

SCREENING OF DIFFERENTIALLY EXPRESSED SEQUENCES BY DOT-BLOT ANALYSIS

Bacterial colony PCR was performed using a GeneAmp PCR System-9700 with 1 μL of bacteria culture in a total PCR volume of 25 μL (400 nM each of NP1 and NP2R primers [Pei et al., 2007], 0.2 mM of each dNTP, 0.5 μL Taq polymerase mix, and 1 × PCR buffer). The forward and reverse subtracted cDNA was digested with RsaI to remove the SSH adapters. The adapter-free cDNA was labeled by a dig high-prime labeling and detection starter kit (Roche Molecular Biochemicals, Mannheim, Germany) using a random priming method. An aliquot (1 μL) of each positive PCR product (10 ng) was dropped onto a nylon membrane (Amersham, Braunschweig, Germany) in duplicate and fixed by irradiation under a UV transilluminator for 8 min. A detailed protocol for hybridization was carried out according to the manufacturer's protocol.

SEQUENCE ANALYSIS

Following dot-blot hybridization, the differentially expressed sequences were sequenced using the M13 primer (Applied Invitrogen, Shanghai, China). Sequencher was used to examine all sequence traces, and all vector and adaptor sequences were removed. Homology searches against GenBank databases were done using the BLAST server (http://www.ncbi,nlm.nih.gov/BLAST/) at the National Center for Biotechnology Information (NCBI). Homologous sequences with no repeats and an *E*-value of less than E-10 over at least a 100-bp stretch were considered identical [Johannessen et al., 2007]. The differentially expressed genes, identified through expression analysis, were classified according to the definition of gene ontology (http://www.geneontology.org/) related to the aspects of biological function, molecular function, and cellular component. When the KEGG was used for automatic annotation, the partial gene sets were used as background, with bidirectional best hit (BBH) as the assignment method (http://www.genome.jp/tools/kaas/). All EST sequences have been submitted to the EST division of GenBank NCBI (http://www.nlm.nih.gov/dbEST/).

QUANTITATIVE PCR

Real-time PCR was performed on samples from hepatocytes treated with FFA mixtures and untreated control hepatocytes. Samples were reverse transcribed using a PrimeScript™ RT system kit for real-time PCR (TaKaRa, Japan) according to the manufacturer's instructions. The SYBR PrimeScript™ RT-PCR Kit (TaKaRa, Japan) and Bio-Rad IQ5 kit (Bio-Rad, Germany) were used for relative quantification of cDNAs through real-time quantitative PCR. The real-time quantitative PCR reaction contained the newly generated cDNA template, SYBR Premix Ex Taq™, sterile water and primers corresponding to the target genes. Real-time PCR was performed on the Cycler system (one cycle of 95°C for 10 s, 40 cycles of 95°C for 5 s, and 60°C for 40 s). An 80-cycle melt curve was performed to determine primer specificity by starting at 55°C and increasing the temperature by 0.5° every 10 s.

Some clones were selected for real-time quantitative PCR analysis on the basis of their possible relevance to alterations in metabolic pathways. The selected clones were sequences showing similarity to the following genes: diacylglycerol O-acyltransferase homolog 1 (DGAT-1), aldolase B (ALDOB), diacylglycerol O-acyltransferase homolog 2 (DGAT-2), dehydrogenase/reductase (SDR family) member 7 (DHRS7), peroxisome proliferator-activated receptor alpha (PPARα), carnitine palmitoyltransferase I (CPT-1), methionine adenosyltransferase I (MAT), inositol hexaphosphate kinase 2 (IHPK2), Acyl-CoA synthetase long-chain family member 3 (ACSL3), apolipoprotein H (apoH), Cell death activator CIDE-3 (CIDEc), acyl-CoA synthetase long-chain family member 1 (ACSL1), kinesin family member 1B (KIF1B), MLX interacting protein-like (ChREBP), phosphoenolpyruvate carboxykinase 1 (PCK), peroxisome proliferator-activated receptor delta (PPARβ), apolipoprotein B (apoB), forkhead box O1A (FoxO1), fatty acid binding protein 4 (A-FABP), and liver basic fatty acid binding protein (L-FABP). The specific primers are listed in Table I.

TABLE I. Primer Sequences for qPCR

Putative gene name	Forward primer	Reverse primer	Product size (bp)
A-FABP	5′- AGGAAGATGGCTGGTGT -3′	5′- TCATCAAACTCTTCACCC -3′	128
ACSL1	5′- TGGAAGTAGAGGGTGGT-3′	5′-CTCATACGGCTGGTTTT -3′	173
ACSL3	5′-CGGGCTCAATGAAACGG -3′	5′-GTCGCAGCAGCGGAACT -3′	98
apoB	5′-CTCAAGCCAACGAAGAA-3′	5′-AGCAAGTCAAGGCAAAA -3′	152
ChREBP	5′-CAAGAAGCGGCTCCGAAAG -3′	5′-GGGCACCACATTGCAGAAGA -3′	118
CPT-1	5′-AGAACAGATGGCGGTCAA-3′	5′-GTCCGTTCATGTACTGTTGA -3′	163
DGAT1	5′-TCCGAGTTCCACCAGTCC-3′	5′-CATCTGGCTCATCTTCTTCTACT-3′	108
DGAT2	5′-CAAAGAAAGGTGGAAGAAG-3′	5′-GTCAGCAGATTGTGGGTT-3′	106
FoxO1	5′-AGTCTGGTCAAGAGGGAA-3′	5′-TGGCTGATGATGGGTAT-3′	225
FSP27	5′-TGGCCTGCATCACTTTCGA-3′	5′-CCGTAGAGCGTGGCTTTGAC-3′	79
ALDOB	5′-TCACCAGCACAACACCC-3′	5′-ACAGCAGCCAGAACCTTT-3′	178
DHRS7	5′-TGGCTGATGAACAGAATG-3′	5′-TTAGTACAAGTAGAGCAGGAAT-3′	109
MAT	5′-CAGCACCAACATCTTCTT-3′	5′-AGCGTGGCTTTGACTA-3′	111
IHPK2	5′-TCATAACGGCAAATACCT-3′	5′-GCCTTTCCTTCCCATC-3′	143
KIF1B	5′-TGTAGAGGTGGCTTGG-3′	5′-CAGTCCTGGGTTTGTTT-3′	105
PCK	5′-GGGATGAGCACAAGGTTC-3′	5′-AGTGATGGCGGTGTCTATT-3′	117
PPARα	5′-AGCATAGATGAATCACCCAG-3′	5′-AACCCTTACAACCTTCACA-3′	109
PPARβ	5′-TGACGGCGAGCGAGAT-3′	5′-CAGGTAGGCGTTGTAGATGTG-3′	83
[a]β-actin	5′-CAACGAGCGGTTCAGGTGT -3′	5′-TGGAGTTGAAGGTGGTCTCGT -3′	92
[a]18S	5′TTGGTGGAGCGATTTGTC3′	5′ATCTCGGGTGGCTGAACG3′	129

[a]Housekeeping gene for data normalization.

The relative expression ratio of target mRNAs was calculated using the Multicolor Real-Time PCR Detection System IQ^{TM}5 software 5.0 (Bio-Rad, USA). The following calculation method was employed: calibrator-normalized relative quantification using the $2^{-\square\square CT}$ method [Livak KJ, 2001]. Ribosomal 18S rRNA and β-actin were used as reference genes. All reactions were done in triplicate, and the data represent the mean of three independent experiments between Landes geese and Sichuan White geese.

STATISTICAL ANALYSIS

The data were subjected to ANOVA testing, and the means were assessed for significance by Tukey's test. Analysis of variance and *t*-tests were performed using the SAS 9.13 package (SAS Institute Inc., Cary, NC). Results are presented as mean ± SD.

RESULTS

CYTOTOXICITY AND CASPASE-3 ACTIVATION IN FFA-OVERLOADED GOOSE HEPATIC

The cytotoxicity of the FFA mixtures at different ratios (oleate/palmitate at 3:0, 2:1, 1:1, 1:2, and 0:3) was investigated after 24 h of treatment. The results indicated that the various ratios of the FFA mixtures produced different cytotoxic effects. As Figure 1 suggested, no cytotoxic effect was observed in goose hepatocytes at the oleate/palmitate ratios of 3:0, 2:1, 1:1, and 1:2 at up to 2 mM, whereas a strong cytotoxic effect was shown at 1.0, 1.5, and 2 mM of the FFA mixture at the 0:3 ratio. These results suggest a cytotoxic-dependent effect of an increase in palmitate concentration in the FFA mixtures.

The activation of caspases-3 was evaluated in goose primary hepatocytes treated with various ratios of oleate/palmitate at 0.5, 1.0, 1.5, and 2.0 mM for 24 h. As shown in Figure 2, caspase-3 activation was markedly increased in cultures treated with the higher ratios of palmitic acid.

TG CONCENTRATION OF GOOSE HEPATIC CELLS WITH DIFFERENT RATIOS OF FFAS

Goose hepatocytes were incubated with 0.5, 1.0, 1.5, and 2.0 mM of the FFA mixtures (oleate/palmitate) at different ratios (3:0, 2:1, 1:1, 1:2, and 0:3) for 24 h. Hepatocytes that were exposed to the FFA mixtures developed a clear dose-dependent increase of TG accumulation in the cytosol. Especially, oleate/palmitate at a 2:1 ratio induced a higher level of intracellular TG concentration. However, as Figure 3 shows, lower TG levels were found in cells treated with palmitate alone (0:3 ratio), as it is apparently toxic at such a concentration.

Therefore, to achieve maximal TG overaccumulation with minimal cytotoxicity, the FFA mixture containing a low proportion of palmitic acid (oleate/palmitate at a 2:1 ratio) was selected for further experiments. As shown in Figure 4, a great quantity of lipid drops accumulated in goose hepatocyte treated with oleate/palmitate at a 2:1 ratio.

PROPERTIES OF THE TWO RECIPROCAL SUBTRACTIVE CDNA LIBRARIES

The basic properties of the SSH-1 and SSH-2 libraries were summarized in Table II. After assembly of the 281 SSH-1 derived sequences, 64 contigs were obtained. These 64 contigs contained two or more expressed sequence tags (ESTs) with an average reading of 4.4. The largest contig was composed of 10 ESTs. The assembly of the 221 SSH-2 ESTs provided 44 contigs that contained at least two ESTs (five on average). The largest contig from SSH-2 contained 11 ESTs. For both libraries, most readings belonging to the same contig

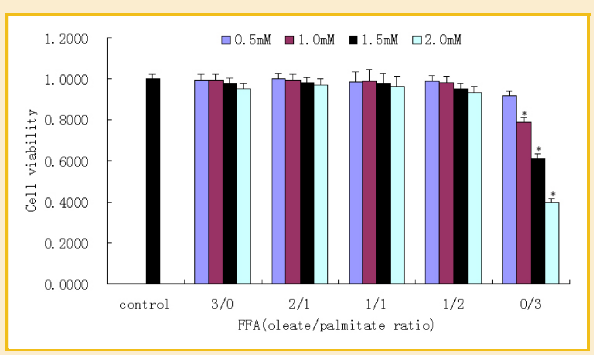

Fig. 1. Cytotoxicity of FFA overloading at different ratios. The cytotoxicity of the FFA mixture at different ratios (oleate/palmitate at 3:0, 2:1, 1:1, 1:2, and 0:3 ratios) was assessed by the MTT test at 24 h after treatment. * $P < 0.05$ in relation to controls. [Color figure can be viewed in the online issue, which is available at wileyonlinelibrary.com.]

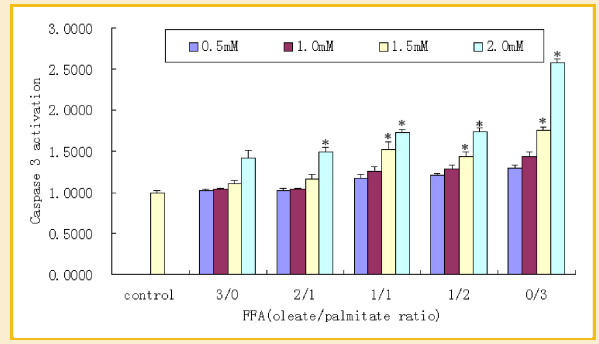

Fig. 2. Caspase-3 activation in FFA-overloaded goose hepatocytes. * $P < 0.05$ in relation to controls. [Color figure can be viewed in the online issue, which is available at wileyonlinelibrary.com.]

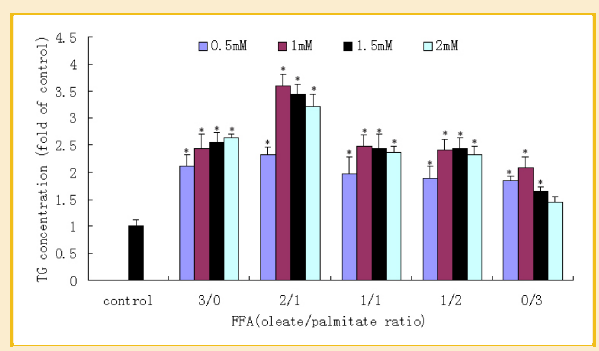

Fig. 3. TG concentration of goose hepatic cells with different FFA ratios. * $P < 0.05$ in relation to controls. [Color figure can be viewed in the online issue, which is available at wileyonlinelibrary.com.]

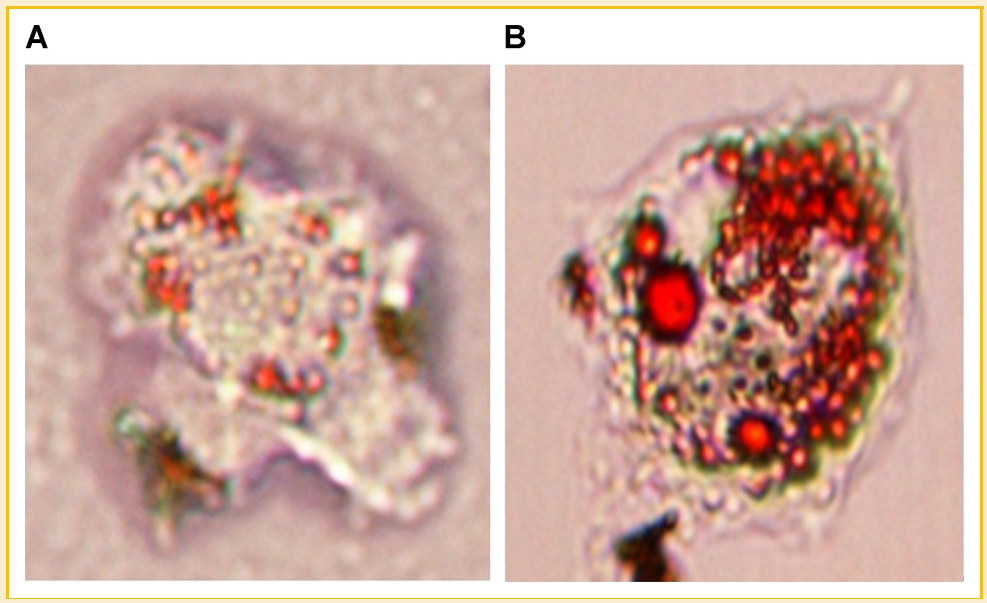

Fig. 4. Lipid drops revealed by oil red O staining. Florescence microscope ×4 200 A: control; B: FFA (oleate/palmitate 2:1 ratio) treatment.

were nearly identical. In fact, the range of length for contigs and ESTs was coincident for both libraries. Sequences representative of the 108 contigs were deposited to the GenBank dbEST under accession numbers GW342904-GW343011.

A blast nucleotide search on the 108 sequences obtained against GenBank databases revealed that 51 and 36 contigs from the SSH-1 and SSH-2 libraries, respectively, aligned perfectly with one or more of the sequences available in the public databases. A total of 21 sequences could not be aligned with any of the available sequences; thus, they were labeled as uncharacterized sequences (see Tables III and V).

GENE ANNOTATION AND PATHWAY IDENTIFICATION

A number of up- and down-regulated ESTs associated with TG concentration were isolated by SSH. The most relevant genes were selected according to their roles in the pathways related to metabolic homeostasis.

Fifty-eight homologous genes were classified in terms of gene ontology. Table V shows the cellular composition of fifteen genes in the cytoplasm, with eight genes in the nucleus and others on the plasma membrane. Their molecular function was identified as catalytic activity, and their biological function was also involved lipid metabolism, ATPase binding and signal transduction. Moreover, two nuclear factors (PPARα and PPARβ) identified in this study are key nuclear factor for lipid metabolism. Genes without specific data available were denoted as ND (Table V).

In addition to these methods, the KEGG Automatic Annotation System (KAAS) (http://www.genome.jp/tools/kaas/) was then used to re-analyze all of the ESTs for orthology assignment and pathway mapping [Geng Hongwei et al., 2008]. The KO identifier confirmed four functional categories (Table VI). The main functional categories were carbohydrate, lipid and energy metabolism, translation and signal transduction. Although 16 genes were assigned KO numbers, 29 genes were distributed in a number of pathways because a gene might have more than one function in different pathways. These genes were involved in 12 pathways, and the most frequent pathways were shown in Table VI. All the pathways are related to lipid metabolism, such as glycolysis, oxidative phosphorylation, ATP synthesis, fatty acid metabolism, PPAR signaling pathway, and the insulin signaling pathway.

TABLE II. Summary of the Contents of the SSH-1 and SSH-2 cDNA Libraries Derived From Landes Geese and Sichuan White Geese Hepatocytes.

	[a]SSH-1	[b]SSH-2	Total
Clones sequenced	300	250	550
Empty plasmids	19	29	48
Sequences obtained	281	221	502
Number of contigs	64	44	108
Sequence length range (bp)	126–793	150–1098	126–1098
Average sequence length (bp)	383	385	384
Novel sequences	13	8	21

[a]SSH-1: cDNA from the control as the "driver" and the cDNA from the hepatocytes of added FFA as the "tester".
[b]SSH-2: cDNA from the control as the "tester" and the cDNA from the hepatocytes of added FFA as the "driver".

GENE EXPRESSION ANALYSIS

Twenty clones were selected, based on their similarity to genes involved in processes such as carbohydrate and lipid metabolism and metabolism signaling pathways. Normalized fold-expression analysis from real-time quantitative PCR data showed that expression of 13 out of the 20 clones tested was significantly higher ($P < 0.05$) in hepatocytes treated with FFAs compared with the control. As Table VII showed, the 13 differentially expressed clones were DGAT-1, ALDOB, DGAT-2, DHRS7, PPARα, CPT-1, MAT, ACSL3, ACSL1, PCK, PPARβ, A-FABP, and L-FABP. The normalized fold expression of ChREBP, apoB, Fox01, KIF1B, and IHPK2 was significantly higher ($P < 0.05$) in hepatocytes of the untreated control group. No significant difference

TABLE III. Identified Sequences From the SSH-1 Library

GenBank ID.	Clone no.	Blast identity	Blast database no.	Identity (%)	*E*-value
GW342904	FA004	Aldolase B, fructose-bisphosphate (ALDOB)	NM_001007977.1	92	3E-123
GW342905	FA007	UDP glucuronosyltransferase 1 family polypeptide A10	XM_421883.2	92	8E-115
GW342906	FA010	ribosomal protein L22 (RPL22)	NM_204141.1	92	5E-81
GW342907	FA013	Similar to HL23 ribosomal protein (RPL23)	XM_418122.2	94	2E-54
GW342908	FA016	heat shock 70kDa protein 5 (HSPA5)	NM_205491.1	92	0
GW342909	FA019	Liver basic fatty acid binding protein (L-FABP)	NM_204634.1	92	1E-72
GW342910	FA022	Fibrinogen alpha chain (FGA)	XM_001232366.1	94	4E-139
GW342911	FA035	Heterogeneous nuclear ribonucleoprotein A3	XM_001233126.1	96	0
GW342912	FA041	Apolipoprotein H (apoH)	XM_415683.2	83	3E-68
GW342913	FA047	Enolase 1 (alpha) (ENO1)	NM_205120.1	95	0
GW342914	FA053	Eukaryotic translation elongation factor 2 (EEF2)	NM_205368.1	91	0
GW342915	FA059	Ribosomal protein SA, transcript variant2 (RPSA)	XM_418817.2	92	4E-78
GW342916	FA065	Heme oxygenase (decycling) 1 (HMOX1)	NM_205344.1	92	2E-62
GW342917	FA071	NADH dehydrogenase 1 alpha subcomplex, 4	XM_001234600.1	90	1E-66
GW342918	FA077	Gallus gallus finished cDNA, clone ChEST493p8	BX932700.1	75	1E-35
GW342919	FA078	Gallus gallus cDNA clone gcag0009.f.22 5prim	BX277382.2	72	2E-17
GW342920	FA087	Chicken mixed tissue Gallus gallus cDNA clone 3GAL_51O08 5'	DN929577.1	81	2E-23
GW342921	FA096	Gallus gallus cDNA clone ChEST285m8 5'	BU481728.1	74	4E-29
GW342922	FA114	Gallus gallus similar to MGC82793 protein	XM_001233999.1	92	4.00E-151
GW342923	FA123	Gallus gallus cysteine-rich, angiogenic inducer, 61	NM_001031563.1	93	8.00E-89
GW342924	FA144	Gallus gallus similar to mannosidase, alpha	XM_420805.2	88	2.00E-112
GW342925	FA150	Dehydrogenase/reductase (SDR family) member 7 (DHRS7)	XM_421423.2	79	9.00E-44
GW342926	FA156	Equus caballus interleukin enhancer binding factor 3, 90kDa	XM_001490966.2	86	7.00E-125
GW342927	FA174	Gallus gallus peroxiredoxin 1, transcript variant 2	XM_001233872.1	94	0.00E+00
GW342928	FA180	Gallus gallus cysteine and glycine-rich protein 2 (CSRP2)	NM_205208.1	92	8.00E-169
GW342929	FA181	Gallus gallus annexin A2 (ANXA2)	NM_205351.1	93	1.00E-99
GW342930	FA184	Pan troglodytes TSC22 domain family 2 (TSC22D2)	XM_001138557.1	70	2.00E-10
GW342931	FA190	Gallus gallus hypothetical LOC423790 (LOC423790)	XM_421662.2	73	7.00E-62
GW342932	FA198	Gallus gallus glyceraldehyde-3-phosphate dehydrogenase	NM_204305.1	94	0.00E+00
GW342933	FA206	Xenopus tropicalis MGC89305 protein (MGC89305)	NM_001007868.1	87	2.00E-53
GW342934	FA238	Bos taurus similar to zinc finger protein 813	XM_001787664.1	96	3.00E-25
GW342935	FA240	Gallus gallus hypothetical LOC416017 (LOC416017)	XM_414360.2	89	0.00E+00
GW342936	FA242	Gallus gallus similar to ribosomal protein L33-like protein	XM_001235163.1	94	7.00E-166
GW342937	FA244	Gallus gallus B-cell CLL/lymphoma 10 (BCL10)	XM_422365.2	82	3.00E-91
GW342938	FA246	Gallus gallus similar to protein phosphatase 2C alpha	XM_421422.2	96	0.00E+00
GW342939	FA247	Gallus gallus serpin peptidase inhibitor, clade E, member 2	NM_001083920.1	92	0.00E+00
GW342940	FA251	Gallus gallus polo-like kinase 2 (Drosophila) (PLK2)	XM_424739.2	94	0
GW342941	FA253	Monodelphis domestica similar to IKAP (LOC100010616)	XM_001362098.1	74	4.00E-118
GW342942	FA261	SKAP55-related protein	XM_418727.2	83	4.00E-78
GW342943	FA401	acyl-CoA synthetase long-chain family member 1	NM_001012578.1	91	2.00E-144
GW342944	FA405	Acyl-CoA synthetase long-chain family member 3	XM_422625.2	93	0
GW342945	FA409	Gallus gallus carnitine palmitoyltransferase I	NM_001012898.1	92	2.00E-127
GW342946	FA417	Bos taurus diacylglycerol O-acyltransferase homolog 1	NM_174693.2	91	0
GW342947	FA264	diacylglycerol O-acyltransferase homolog 2	XM_002187633.1	96	4.00E-87
GW342948	FA044	Gallus gallus phosphoenolpyruvate carboxykinase 1	NM_205471.1	90	2e-91
GW342949	FA328	Peroxisome proliferator-activated receptor delta	XM_002199056.1	95	1e-161
GW342950	FA133	Peroxisome proliferator-activated receptor alpha	XM_001236111.1	95	0
GW342951	FA015	Gallus gallus fatty acid binding protein 4, adipocyte	NM_204290.1	98	1e-119
GW342952	FA457	Gallus gallus methionine adenosyltransferase I	XM_421512.1	92	0
GW342953	FA378	Gallus gallus cDNA clone 4o17r2, mRNA sequence	lcl|6986AJ732064.1	95	0
GW342954	FA381	Embryonic gonadal PGC cDNA Library Gallus gallus cDNA 5'	DR411471.1	75	6E-68
GW342955	FA576	No significant similarity found			
GW342956	FA583	No significant similarity found			
GW342957	FA500	No significant similarity found			
GW342958	FA214	No significant similarity found			
GW342959	FA220	No significant similarity found			
GW342960	FA226	No significant similarity found			
GW342961	FA232	No significant similarity found			
GW342962	FA249	No significant similarity found			
GW342963	FA187	No significant similarity found			
GW342964	FA135	No significant similarity found			
GW342965	FA470	No significant similarity found			
GW342966	FA337	No significant similarity found			
GW342967	FA542	No significant similarity found			

of expression level between geese hepatocytes was observed for apoH (apolipoprotein H).

DISCUSSION

The hallmark of hepatic steatosis in goose hepatocytes is that a large proportion of the TG is stored in the hepatocytes with functional integrity [Hermier et al., 1988; Pilo and George, 1983]. In the present study, in which we characterized a hepatic in vitro model of cellular steatosis with TG overaccumulation, various intracellular levels of TG overaccumulation were achieved in goose hepatocytes by overloading cells with various proportions of oleic acid and palmitic acid, and the viability of treated hepatocytes and the activation of caspases-3 were significantly altered (Figs. 1, 2, 3, and 4). In mammals, studies have shown that monounsaturated

TABLE IV. Identified Sequences From the SSH-2 Library

GenBank ID.	Clone no.	Blast identity	Blast database no.	Identity (%)	*E*-value
GW342968	FA280	Transglutaminase 3 TGM3	XM_417392.2	89	1E-125
GW342969	FA288	Ribosomal protein L39 (RPL39)	NM_204272.1	91	7E-53
GW342970	FA292	Hypothetical LOC416017	XM_414360.2	89	0
GW342971	FA300	Annexin A2 (ANXA2)	NM_001030801.1	93	4E-97
GW342972	FA308	ash2 (absent, small, or homeotic)-like (ASH2L)	NM_001031395.1	90	2E-48
GW342973	FA316	Ribosomal protein S4, X-linked (RPS4X)	NM_205108.1	94	1E-84
GW342974	FA317	Hypothetical LOC423790	XM_421662.2	88	1E-36
GW342975	FA325	Cytochrome c oxidase subunit VIIb (LOC771947)	XM_001235157.1	84	1E-48
GW342976	FA333	Cysteine and glycine-rich protein 2 (CSRP2)	NM_205208.1	92	0
GW342977	FA349	LOC422090 (LOC422090)	NM_001006423.1	89	4E-67
GW342978	FA351	Stem cell antigen 2 (LOC420301)	XM_418413.2	88	5E-57
GW342979	FA353	Otokeratin (LOC395772)	NM_204932.1	90	5E-43
GW342980	FA355	Ribosomal protein L5 (RPL5)	NM_204581.4	95	0
GW342981	FA360	Sorting nexin family member 27 (SNX27)	NM_001031346.1	94	4E-150
GW342982	FA364	Thrombospondin 1 (THBS1)	XM_421205.2	88	9E-93
GW342983	FA368	Inositol hexaphosphate kinase 2 (IHPK2)	NM_001030596.2	94	1E-165
GW342984	FA218	Gallus gallus apolipoprotein B	NM_001044633.1	90	1.00E-160
GW342985	FA073	Equus caballus similar to Cell death activator CIDE-3	XM_002192361.1	86	3.00E-117
GW342986	FA459	Gallus gallus forkhead box O1 (FoxO1)	NM_204328.1	95	1e-167
GW342987	FA580	Gallus gallus MLX interacting protein-like (MLXIPL)	NM_001110841.1	92	0
GW342988	FA428	Gallus gallus calpain 1 (mu/I) large subunit (CAPN1)	NM_205303.1	93	0
GW342989	FA434	Gallus gallus similar to laminin alpha 3 splice variant b1	XM_426078.2	93	2.00E-26
GW342990	FA440	Gallus gallus similar to KIAA0342 protein (LOC420728)	XM_418827.2	92	3.00E-86
GW342991	FA448	Gallus gallus filamin A interacting protein 1 (FILIP1)	XM_419877.2	94	5.00E-152
GW342992	FA467	Gallus gallus complement component 3 (C3)	NM_205405.1	84	0
GW342993	FA495	Gallus gallus hypothetical LOC426122 (LOC426122)	XM_430363.2	84	7.00E-16
GW342994	FA501	Gallus gallus B-cell translocation gene 1, anti-proliferative	NM_205350.1	95	0
GW342995	FA507	Taeniopygia guttata cullin 2 (LOC100221330) mRNA	XM_002194576.1	96	0.00E + 00
GW342996	FA513	Gallus gallus hypothetical LOC416572 (LOC416572)	XM_414873.2	80	7.00E-107
GW342997	FA534	Gallus gallus kinesin family member 1B (KIF1B)	XM_417608.2	94	0
GW342998	FA555	Gallus gallus RNA binding motif protein 5 (RBM5)	NM_001012780.1	93	4.00E-154
GW342999	FA471	Gallus gallus gephyrin (GPHN)	NM_001031549.1	95	0
GW343000	FA384	Gallus gallus cDNA clone gcal0014.o.17	BX264777.3	76	1E-34
GW343001	FA387	Gallus gallus cDNA 5', mRNA sequence	lcl|29613CO761468.1	87	0
GW343002	FA390	Anas platyrhynchos cDNA clone duckAP26_3H12 5'	lcl|25574DR765990.1	92	5E-99
GW343003	FA393	Anas platyrhynchos cDNA clone duck AP26_7G12 5'	lcl|3764DR783187.1	85	5E-93
GW343004	FA431	No significant similarity found			
GW343005	FA437	No significant similarity found			
GW343006	FA456	No significant similarity found			
GW343007	FA366	No significant similarity found			
GW343008	FA479	No significant similarity found			
GW343009	FA567	No significant similarity found			
GW343010	FA268	No significant similarity found			
GW343011	FA445	No significant similarity found			

oleic acid is less toxic than palmitic acid in preventing hepatocytes' toxicity in in vitro steatosis models, and oleic acid is more steatogenic but less cytotoxic than palmitic acid in hepatocyte cell cultures. However, given the previously reported increased levels of fat resulting from the incubation of the two fatty acids combined [Gomez-Lechon et al., 2007; Listenberger et al., 2003; Ricchi et al., 2009], which was similar to our results, the combination of oleic and palmitic acids appears more efficient than the use of either acid individually, and oleic acid is less cytotoxic than palmitic acid in goose hepatocytes (Figs. 1 and 2). Therefore, the FFA mixture containing a low proportion of palmitic acid (oleate/palmitate at a 2:1 ratio) was selected for construction of the cDNA library by SSH.

SSH has been widely used to screen differentially expressed genes in various kinds of cell studies [Diatchenko et al., 1996; Thais Martins de Lima et al., 2004; Cortes et al., 2008]. The goal of this study was to identify up- and down-regulated levels of gene expression in hepatocytes through the addition of FFA mixtures. The detection of differentially expressed genes could aid in elucidating the molecular mechanisms associated with goose hepatic steatosis. A number of differentially expressed genes were successfully identified by SSH and real-time quantitative PCR. These identified genes play important roles in lipid metabolism, such as de novo synthesis, TG synthesis, lipid droplet accumulation, and secretion. Interestingly, some genes involved in TG synthesis, lipid droplet accumulation and FA oxidation were more highly expressed in hepatocytes treated with FFA than in untreated control hepatocytes. However, some genes involved in de novo synthesis and secretion were more highly expressed in untreated control hepatocytes (Tables V and VII). Also, several transcription factors (TFs) were more highly expressed in hepatocytes treated with FFA. It might be that the hepatocellular steatosis of geese has relevance to some metabolic pathways.

Further experiments of our study indicated that multiple genes and multiple pathways might be involved in an FFA stress responses in hepatocyte. The KEGG pathway database is a collection of manually drawn pathway maps based on extensive survey of published literature, allowing the description of general biochemical reactions and their relationships [Thais Martins de Lima et al., 2004; Moriya et al., 2007]. Based on the pathway information obtained from the KEGG, some ESTs involved in important pathways were identified.

Hepatic steatosis development results from an accumulation of triacylglycerol in the liver, and lipid droplets are the storage mode of

TABLE V. Classification of Up- and Down-regulated Genes in SSH Library

Gene	Cellular component	Biological process	Molecular function
ALDOB	Microtubule organizing center	Metabolic process	ATPase binding
RPL22	Ribosome	Translation	Heparin binding
RPL23	Cytoplasm	Translational elongation	Structural constituent of ribosome
HSPA5	Endoplasmic reticulum	Cellular response to glucose starvation	ATP binding
L-FABP	Cytoplasm	Phosphatidylcholine biosynthetic process	Lipid binding
HNRA3	Ribonucleoprotein complex	mRNA processing	Nucleic acid binding
apoH	Extracellular region	Regulation of blood coagulation	Heparin binding
ENO1	Cytoplasm	Glycolysis	Lyase activity
EEF2	Cytoplasm	Translation	GTPase activity
RPSA	Cytoplasm	Translation	Structural constituent of ribosome
HMOX1	Nucleus	Oxidation reduction	Signal transducer activity
NDUFA4	Mitochondrion	Electron transport chain	ND[a]
CRAI61	Extracellular region	Regulation of cell growth	Insulin-like growth factor binding
mannosidase	Golgi apparatus	Protein amino acid N-linked glycosylation	Calcium ion binding
DHRS7	ND[a]	Oxidation reduction	Catalytic activity
ILF3	Intracellular	Regulation of transcription	DNA binding
peroxiredoxin	Mitochondrion	Oxidation reduction	Antioxidant activity
CSRP2	Nucleus	Cell differentiation	Metal ion binding
ANXA2	Cytoplasm	Angiogenesis	Phospholipase inhibitor activity
TSC22D2	ND[a]	Regulation of transcription, DNA-dependent	Transcription factor activity
GAPDH	Mitochondrion	Metabolic process	Oxidoreductase activity
RPL33	Ribosome	Translation	Heparin binding
BCL10	Cytoplasm	Induction of apoptosis	NF-kappaB binding
phosphatase 2C	ser/pro phosphatase complex	Amino acid dephosphorylation	Catalytic activity
PLK2	ND[a]	Amino acid phosphorylation	ATP binding
IKAP	Cytoplasm	Transcription	Protein binding
SKAP55	Cytoplasm	Immune response	Protein kinase binding
ACSL1	Integral to membrane	Lipid metabolic process	Catalytic activity
ACSL3	Membrane	Lipid metabolic process	Catalytic activity
CPT-1	Mitochondrion	Fatty acid beta-oxidation	Acyltransferase activity
DGAT1	Endoplasmic reticulum	Triglyceride biosynthetic process	Diacylglycerol O-acyltransferase activity
DGAT2	Endoplasmic reticulum	Triglyceride biosynthetic process	Diacylglycerol O-acyltransferase activity
PCK	Magnesium binding	Lipid metabolism	Cytoplasm
PPARβ	Nucleus	Fatty acid metabolic process	Transcription factor activity
PPARα	Nucleus	Fatty acid metabolic process	Transcription factor activity
A-FABP	Cytoplasm	Phosphatidylcholine biosynthetic process	Lipid binding
MAT	ND[a]	One-carbon metabolic process	Metal ion binding
TGM3	Cornified envelope	Skin development	Acyltransferase activity
RPL39	Mitochondrion	Translation	Structural constituent of ribosome
ANXA2	Cytoplasm	Angiogenesis	Calcium ion binding
ASH2L	Histone methyltransferase complex	Regulation of transcription	Zinc ion binding
RPS4X	Multicellular organismal development	Cytoplasm	Structural constituent of ribosome
CSRP2	Nucleus	Cell differentiation	Metal ion binding
RPL5	Large ribosomal subunit	ND[a]	Structural constituent of ribosome
SNX27	Cytoplasm	Cell communication	Phosphoinositide binding
THBS1	Extracellular space	Inflammatory response	Calcium ion binding
IHPK2	Nucleus	Phosphoinositide phosphorylation	ATP binding
apoB	Extracellular region	Regulation of blood coagulation	Heparin binding
CIDE-c	Cytoplasm	Induction of apoptosis	Protein binding
FoxO1	Nucleus	Insulin receptor signaling pathway	Protein binding
ChREBP	Cytoplasm	Glucose homeostasis	Transcription factor binding
CAPN1	Cytoplasm	Proteolysis	Hydrolase activity
LAMA3	Extracellular region	Regulation of cell migration	Receptor binding
BTG1	Nucleus	Positive regulation of catalytic activity	Protein binding
cullin 2	Protein catabolic process	Cullin-RING ubiquitin ligase	Protein binding
KIF1B	Cytoplasmic vesicle	Mitochondrion transport along microtubule	ATPase activity
RBM5	Intracellular	Apoptosis	Metal ion binding
GPHN	Plasma membrane	Molybdopterin cofactor biosynthetic process	Catalytic activity

[a]ND: No biological data available.

triacylglycerol [Hermier et al., 1994; Fong et al., 2000]. Peroxisome proliferator-activated receptors (PPARs) are lipid-activated TFs that belong to the steroid/thyroid/retinoic acid receptor superfamily; the PPAR family encompasses PPARα, PPARβ, and PPARγ. All of their characterized target genes encode proteins that participate in lipid homeostasis [Lemberger et al., 1996; Duplus et al., 2000]. In the present study, we found that the expression of goose PPARα and PPARβ was increased by treatment with FFA mixtures, by 111% and 40%, respectively. Moreover, we also found several genes involved in the PPAR signaling pathway, such as A-FABP (GenBank accession no. GW342951), L-FABP (GenBank accession no. GW342909), PCK (GenBank accession no. GW342948), CPT-1 (GenBank accession no. GW342945), ACSL3 (GenBank accession no. GW342944), and ACSL1 (GenBank accession no. GW342943). The PPARα and PPARβ activators are well-known for regulating genes involved in the uptake, transport and metabolism of fatty acids, and activation of fatty acids into acyl-CoA is required for further metabolism of fatty acids, including incorporation into TGs and fatty-acid oxidation [Wahli et al., 1999; Chakrabarti et al., 2003; Edvardsson et al., 2006; Bedu et al., 2007; Fan et al., 2009]. CPT-1 is a key enzyme of fatty acid beta-oxidation; it regulates long-chain fatty acid (LCFA) entry into mitochondria, where the LCFAs undergo

TABLE VI. Main Pathway Identified by KEGG Automatic Annotation System (KAAS)

Pathway	Pathway no.	Genes involved
Metabolism		
Carbohydrate metabolism	ko00010, ko00020,ko00620	GW342948, GW342987
Energy metabolism		
Oxidative phosphorylation	ko00190	GW342945, GW342925
ATP synthesis	ko00193	GW342940, GW342908
Lipid metabolism		
Fatty acid metabolism	ko00071	GW342943, GW342944, GW342912, GW342984
Glycerolipid metabolism	ko00561	GW342946, GW342947
Retinol metabolism	ko00830	GW342946, GW342947
Lipoic acid metabolism	ko00785	GW342982
Signal transduction		
Insulin signaling pathway	ko04910,	GW342948, GW342986, GW342987
PPAR signaling pathway	ko03320,	GW342909, GW342948, GW342945, GW342949, GW342944, GW342943, GW342950, GW342951
Adipocytokine signaling pathway	ko04920,	GW342945, GW342943, GW342944, GW342948

beta-oxidation [Obici et al., 2003], ACSL1 is the major isoform responsible for activating LCFA for fatty acid beta-oxidation [de Jong et al., 2007], and L-FABP and A-FABP also take part in fatty-acid oxidation [Nagasawa et al., 2006; Newberry et al., 2008]. This experimental result showed that the expression of goose CPT-1, ACSL1, L-FABP, and A-FABP was upregulated by FFA mixture treatments, by 105%, 54%, 134%, and 40%, respectively. This result implies that fatty acid beta-oxidation was increased, which is consistent with a PPAR agonist improving hepatic steatosis via an improvement in fatty acid beta-oxidation and a direct prevention of inflammation [Nagasawa et al., 2006]. Furthermore, ACSL3, a lipid droplet-correlation protein, was also upregulated by FFA mixture treatments in goose hepatocyte, which is coincident with oil red O staining expression (Fig. 3). However, FSP27, anther lipid droplet-correlation protein and a direct mediator of PPARγ-dependent hepatic steatosis in mouse hepatocytes [Matsusue et al., 2008; Liu et al., 2009], was downregulated by FFA mixture treatments. This result implies that FSP27 (CIDEc) has a different function in birds, but the mechanics still need to be investigated.

New synthesized TG could be either assembled with one apoB molecule to form VLDL (a lipoprotein rich in TG) or transiently stored as lipid droplets in the cytosol. Fatty liver in the goose results from an increased hepatic lipogenesis in response to overfeeding, together with a deficient secretion of triacylglycerol as VLDL [Hermier et al., 1994; Han et al., 2009]. In the present study, we found that the expression of goose forkhead box O1 (FoxO1, GenBank accession no. GW342986) and carbohydrate-responsive element-binding protein (ChREBP, GenBank accession no. GW342987), two TFs that play key roles in hepatic insulin signaling [Uyeda et al., 2002; Munoz et al., 2006; Kamagate et al., 2008], were remarkably suppressed by FFA mixture treatments. ChREBP is able to control transcription of lipogenic enzyme genes in response to nutritional and hormonal inputs and may play an important role in disease states, such as diabetes, obesity, and hepatic steatosis [Dentin et al., 2005; Denechaud et al., 2008]. Our results suggested that TG overaccumulation in goose hepatocyte caused the expression of ChREBP to decrease. These results indicate that the de novo synthesis of fatty acids was inhibited, which is consistent with the result that insulin and glucose may affect hepatic lipogenesis by regulating lipogenic gene expression and lipogenic enzyme activity in goose hepatocytes [Han et al., 2009]. The forkhead TF FoxO1 acts in the liver to integrate hepatic insulin action and VLDL production. Augmented FoxO1 activity in insulin-resistant livers promotes hepatic VLDL overproduction and predisposes hepatocytes to the

TABLE VII. Quantified Up- and Down-regulated Gene-expression Levels of Selected Clones

GenBank ID.	Homologous gene	Controlled mean ± SD	Treatment mean ± SD
GW342987	ChREBP	1 ± 0.0377	0.517 ± 0.028*
GW342986	FoxO1	1 ± 0.0376	0.423 ± 0.025**
GW342984	apoB	1 ± 0.0389	0.71 ± 0.053*
GW342947	DGAT-2	1 ± 0.029	1.929 ± 0.096**
GW342946	DGAT-1	1 ± 0.032	1.39 ± 0.079*
GW342948	PCK	1 ± 0.027	1.446 ± 0.062*
GW342943	ACSL1	1 ± 0.039	1.54 ± 0.066**
GW342904	ALDOB	1 ± 0.039	2.108 ± 0.0998**
GW342925	DHRS7	1 ± 0.038	1.454 ± 0.076*
GW342952	MAT	1 ± 0.032	1.461 ± 0.076*
GW342983	IHPK2	1 ± 0.063	0.684 ± 0.026*
GW342997	KIF1B	1 ± 0.055	0.716 ± 0.027*
GW342944	ACSL3	1 ± 0.028	1.788 ± 0.086**
GW342950	PPARα	1 ± 0.031	2.112 ± 0.128**
GW342949	PPARβ	1 ± 0.033	1.407 ± 0.036*
GW342951	A-FABP	1 ± 0.021	1.682 ± 0.042**
GW342909	L-FABP	1 ± 0.026	2.34 ± 0.135**
GW342912	apoH	1 ± 0.014	0.925 ± 0.02
GW342945	CPT-1	1 ± 0.038	2.047 ± 0.092**
GW342985	FSP27	1 ± 0.034	0.7 ± 0.043*

* Denotes a significant difference in treatments ($P < 0.05$); whereas ** denotes a significant difference in treatments ($P < 0.01$).

development of hypertriglyceridemia [Kamagate and Dong, 2008; Wang et al., 2009]. We found that the expression of goose apolipoprotein B (apoB, GenBank accession no. GW342984) was also decreased in goose hepatocyte with TG overaccumulation, which indicates that it FoxO1 may be inhibited and excluded from the nucleus, resulting in the inhibition of hepatic MTP (microsomal triglyceride transfer protein) and apoB expression. This activity abates VLDL production and limits postprandial TG excursion, which is supported by Han et al. studies [Han Chun-chun et al., 2008].

Acyl-CoA:diacylglycerol acyltransferases (DGATs) are enzymes that catalyze the formation of TG from acyl-CoA and diacylglycerol. Two DGATs have been identified, which belong to two distinct gene families [Shi and Cheng, 2009]. In our present study, TG deposition in goose hepatocyte was induced through treatment with an FFA mixture (oleate/palmitate at a 2:1 ratio), and DGAT1 (GenBank acc. no. GW342946) and DGAT2 (GenBank acc. no. GW342947) were significantly upregulated. Studies in mouse primary hepatocytes indicated that DGAT1 deficiency protected against hepatic steatosis by reducing the synthesis and increasing the oxidation of fatty acids, and knockdown of DGAT2 with antisense oligonucleotide reduces VLDL-TG and ApoB secretion in mice [Liu et al., 2008; Villanueva et al., 2009]. The present study demonstrated that the mRNA abundance of DGAT2 in goose primary hepatocytes treated with FFAs had significant positive correlations with the hepatocytes' TG content, although DGAT1 expression did not exhibit such a correlation (data not shown). These data indicated that DGATs might play different roles in hepatosteatosis of geese.

In two SSH libraries, with the exception of genes belonging to metabolism pathways, twenty-one genes were not found to have significant similarity in NCBI databases. Further investigation currently being conducted by our group should reveal the characteristic of these genes and their possible role in FFA-regulated processes in the goose.

Collectively, these results show that goose hepatocytes are induced to over accumulate fat by a mixture of FFA (oleate/palmitate at a 2:1 ratio) that is associated with minor toxic and apoptotic effects, thus representing a cellular model of steatosis for researching molecular mechanisms of hepatic steatosis in the bird. Suppressive subtractive hybridization and real-time PCR techniques identified genes that play important roles in lipid metabolism, including de novo synthesis, TG synthesis, lipid droplet accumulation, and secretion. These studies indicate that a mixtures of oleic and palmitic acids (oleate/palmitate at a 2:1 ratio) could induce hepatic steatosis without sacrificing cellular function, which may upregulate TG synthesis-relevant genes expression and suppress assembly and secretion of VLDL-TGs. Meanwhile, treatment with FFA mixtures may increase fatty-acid oxidation to maintain the appropriate mass and function of goose primary hepatocytes.

ACKNOWLEDGMENTS

The work was supported by the National Waterfowl Industrial Technology System (No. nycytx-45-05) and the Research Fund for the Doctoral Program of Higher Education (No. 200806260005).

REFERENCES

Bedu E, Desplanches D, Pequignot J, Bordier B, Desvergne B. 2007. Double gene deletion reveals the lack of cooperation between PPARalpha and PPARbeta in skeletal muscle. Biochem Biophys Res Commun 357:877–881.

Bradbury MW. 2006. Lipid metabolism and liver inflammation. I. Hepatic fatty acid uptake: Possible role in steatosis. Am J Physiol Gastrointest Liver Physiol 290:G194–G198.

Chakrabarti R, Vikramadithyan RK, Misra P, Hiriyan J, Raichur S, Damarla RK, Gershome C, Suresh J, Rajagopalan R. 2003. Ragaglitazar: A novel PPAR alpha PPAR gamma agonist with potent lipid-lowering and insulin-sensitizing efficacy in animal models. Br J Pharmacol 140:527–537.

Cortes T, Tagu D, Simon JC, Moya A, Martinez-Torres D. 2008. Sex versus parthenogenesis: A transcriptomic approach of photoperiod response in the model aphid Acyrthosiphon pisum (Hemiptera: Aphididae). Gene 408:146–156.

de Jong H, Neal AC, Coleman RA, Lewin TM. 2007. Ontogeny of mRNA expression and activity of long-chain acyl-CoA synthetase (ACSL) isoforms in Mus musculus heart. Biochim Biophys Acta 1771:75–82.

den Boer M, Voshol PJ, Kuipers F, Havekes LM, Romijn JA. 2004. Hepatic steatosis: A mediator of the metabolic syndrome. Lessons from animal models. Arterioscler Thromb Vasc Biol 24:644–649.

Denechaud PD, Girard J, Postic C. 2008. Carbohydrate responsive element binding protein and lipid homeostasis. Curr Opin Lipidol 19:301–306.

Dentin R, Girard J, Postic C. 2005. Carbohydrate responsive element binding protein (ChREBP) and sterol regulatory element binding protein-1c (SREBP-1c): Two key regulators of glucose metabolism and lipid synthesis in liver. Biochimie 87:81–86.

Diatchenko L, Lau YF, Campbell AP, Chenchik A, Moqadam F, Huang B, Lukyanov S, Lukyanov K, Gurskaya N, Sverdlov ED, Siebert PD. 1996. Suppression subtractive hybridization: A method for generating differentially regulated or tissue-specific cDNA probes and libraries. Proc Natl Acad Sci USA 93:6025–6030.

Donato MT, Lahoz A, Jimenez N, Perez G, Serralta A, Mir J, Castell JV, Gomez-Lechon MJ. 2006. Potential impact of steatosis on cytochrome P450 enzymes of human hepatocytes isolated from fatty liver grafts. Drug Metab Dispos 34:1556–1562.

Dowman JK, Tomlinson JW, Newsome PN. 2010. Pathogenesis of non-alcoholic fatty liver disease. QJM 103:71–83.

Duplus E, Glorian M, Forest C. 2000. Fatty acid regulation of gene transcription. J Biol Chem 275:30749–30752.

Edvardsson U, Ljungberg A, Linden D, William-Olsson L, Peilot-Sjogren H, Ahnmark A, Oscarsson J. 2006. PPARalpha activation increases triglyceride mass and adipose differentiation-related protein in hepatocytes. J Lipid Res 47:329–340.

Fan B, Ikuyama S, Gu JQ, Wei P, Oyama J, Inoguchi T, Nishimura J. 2009. Oleic acid-induced ADRP expression requires both AP-1 and PPAR response elements, and is reduced by Pycnogenol through mRNA degradation in NMuLi liver cells. Am J Physiol Endocrinol Metab 297:E112–E123.

Fong DG, Nehra V, Lindor KD, Buchman AL. 2000. Metabolic and nutritional considerations in nonalcoholic fatty liver. Hepatology 32:3–10.

Fossati P, Prencipe L. 1982. Serum triglycerides determined colorimetrically with an enzyme that produces hydrogen peroxide. Clin Chem 28:2077–2080.

Fournier E, Peresson R, Guy G, Hermier D. 1997. Relationships between storage and secretion of hepatic lipids in two breeds of geese with different susceptibility to liver steatosis. Poult Sci 76:599–607.

Geng HW, Shi L, Li W, Zhang B, Chu CC, Li HJ, Genfa Z. 2008. Gene expression of jojoba (Simmondsia chinensis) leaves exposed to dryin. Environ Exp Bot 63:137–146.

Gomez-Lechon MJ, Ponsoda X, O'Connor E, Donato T, Castell JV, Jover R. 2003. Diclofenac induces apoptosis in hepatocytes by alteration of mito-

chondrial function and generation of ROS. Biochem Pharmacol 66:2155–2167.

Gomez-Lechon MJ, Donato MT, Martinez-Romero A, Jimenez N, Castell JV, O'Connor JE. 2007. A human hepatocellular in vitro model to investigate steatosis. Chem Biol Interact 165:106–116.

Han C, Wang J, Li L, Zhang Z, Wang L, Pan Z. 2009. The role of insulin and glucose in goose primary hepatocyte triglyceride accumulation. J Exp Biol 212:1553–1558.

Han CC, Wang JW, Xu HY, Li L, Ye JQ, Zhou WH. 2008. Effect of overfeeding on plasma parameters and mRNA expression of genes associated with hepatic lipogenesis in geese. Aslan-Aust J Anim Sci 21:590–595.

Hermier D, Forgez P, Laplaud PM, Chapman MJ. 1988. Density distribution and physicochemical properties of plasma lipoproteins and apolipoproteins in the goose, Anser anser, a potential model of liver steatosis. J Lipid Res 29:893–907.

Hermier D, Rousselot-Pailley D, Peresson R, Sellier N. 1994. Influence of orotic acid and estrogen on hepatic lipid storage and secretion in the goose susceptible to liver steatosis. Biochim Biophys Acta 1211:97–106.

Johannessen MK, Skretting G, Ytrehus B, Roed KH. 2007. Neonatal growth cartilage: Equine tissue specific gene expression. Biochem Biophys Res Commun 354:975–980.

Kamagate A, Dong HH. 2008. FoxO1 integrates insulin signaling to VLDL production. Cell Cycle 7:3162–3170.

Kamagate A, Qu S, Perdomo G, Su D, Kim DH, Slusher S, Meseck M, Dong HH. 2008. FoxO1 mediates insulin-dependent regulation of hepatic VLDL production in mice. J Clin Invest 118:2347–2364.

Lemberger T, Desvergne B, Wahli W. 1996. Peroxisome proliferator-activated receptors: A nuclear receptor signaling pathway in lipid physiology. Annu Rev Cell Dev Biol 12:335–363.

Listenberger LL, Han X, Lewis SE, Cases S, Farese RV Jr, Ory DS, Schaffer JE. 2003. Triglyceride accumulation protects against fatty acid-induced lipotoxicity. Proc Natl Acad Sci USA 100:3077–3082.

Liu Y, Millar JS, Cromley DA, Graham M, Crooke R, Billheimer JT, Rader DJ. 2008. Knockdown of acyl-CoA:diacylglycerol acyltransferase 2 with antisense oligonucleotide reduces VLDL TG and ApoB secretion in mice. Biochim Biophys Acta 1781:97–104.

Liu K, Zhou S, Kim JY, Tillison K, Majors D, Rearick D, Lee JH, Fernandez-Boyanapalli RF, Barricklow K, Houston MS, Smas CM. 2009. Functional analysis of FSP27 protein regions for lipid droplet localization, caspase-dependent apoptosis, and dimerization with CIDEA. Am J Physiol Endocrinol Metab 297:E1395–E1413.

Livak KJ. 2001. Analysis of relative gene expression data using real-time quantitative PCR and the 2(-delta delta C(T)) method. Methods 25:402–408.

Malhi H, Bronk SF, Werneburg NW, Gores GJ. 2006. Free fatty acids induce JNK-dependent hepatocyte lipoapoptosis. J Biol Chem 281:12093–12101.

Matsusue K, Kusakabe T, Noguchi T, Takiguchi S, Suzuki T, Yamano S, Gonzalez FJ. 2008. Hepatic steatosis in leptin-deficient mice is promoted by the PPARgamma target gene Fsp27. Cell Metab 7:302–311.

Miller TA, LeBrasseur NK, Cote GM, Trucillo MP, Pimentel DR, Ido Y, Ruderman NB, Sawyer DB. 2005. Oleate prevents palmitate-induced cytotoxic stress in cardiac myocytes. Biochem Biophys Res Commun 336:309–315.

Molette C, Berzaghi P, Zotte AD, Remignon H, Babile R. 2001. The use of near-infrared reflectance spectroscopy in the prediction of the chemical composition of goose fatty liver. Poult Sci 80:1625–1629.

Moriya Y, Itoh M, Okuda S, Yoshizawa AC, Kanehisa M. 2007. KAAS: An automatic genome annotation and pathway reconstruction server. Nucleic Acids Res 35:W182–W185.

Munoz MC, Argentino DP, Dominici FP, Turyn D, Toblli JE. 2006. Irbesartan restores the in-vivo insulin signaling pathway leading to Akt activation in obese Zucker rats. J Hypertens 24:1607–1617.

Nagasawa T, Inada Y, Nakano S, Tamura T, Takahashi T, Maruyama K, Yamazaki Y, Kuroda J, Shibata N. 2006. Effects of bezafibrate, PPAR pan-agonist, and GW501516, PPARdelta agonist, on development of steatohepatitis in mice fed a methionine- and choline-deficient diet. Eur J Pharmacol 536:182–191.

Natali F, Siculella L, Salvati S, Gnoni GV. 2007. Oleic acid is a potent inhibitor of fatty acid and cholesterol synthesis in C6 glioma cells. J Lipid Res 48:1966–1975.

Newberry EP, Kennedy SM, Xie Y, Sternard BT, Luo J, Davidson NO. 2008. Diet-induced obesity and hepatic steatosis in L-Fabp/mice is abrogated with SF, but not PUFA, feeding and attenuated after cholesterol supplementation. Am J Physiol Gastrointest Liver Physiol 294:G307–G314.

Obici S, Feng Z, Arduini A, Conti R, Rossetti L. 2003. Inhibition of hypothalamic carnitine palmitoyltransferase-1 decreases food intake and glucose production. Nat Med 9:756–761.

Pei DS, Sun YH, Chen SP, Wang YP, Hu W, Zhu ZY. 2007. Identificatially expressed genes from the cross-subfamily cloned embryos derived from zebrafish nuclei and rare minnow enucleated eggs. Theriogenology 68:1282–1291.

Pilo B, George JC. 1983. Diurnal and seasonal variation in liver glycogen and fat in relation to metabolic status of liver and m. pectoralis in the migratory starling, Sturnus roseus, wintering in India. Comp Biochem Physiol A Comp Physiol 74:601–604.

Ricchi M, Odoardi MR, Carulli L, Anzivino C, Ballestri S, Pinetti A, Fantoni LI, Marra F, Bertolotti M, Banni S, Lonardo A, Carulli N, Loria P. 2009. Differential effect of oleic and palmitic acid on lipid accumulation and apoptosis in cultured hepatocytes. J Gastroenterol Hepatol 24:830–840.

Seglen PO. 1976. Preparation of isolated rat liver cells. Methods Cell Biol 13:29–83.

Shi Y, Cheng D. 2009. Beyond triglyceride synthesis: The dynamic functional roles of MGAT and DGAT enzymes in energy metabolism. Am J Physiol Endocrinol Metab 297:E10–E18.

Thais Martins de Lima, Leonardo de Oliveira Rodrigues, Mario Henrique Bengtson, Mari Cleide Sogayar, Camila Nogueira Alves Bezerra, Nancy Amaral Rebouc as, Curi. R. 2004. Identification of genes regulated by oleic acid in Jurkat cells by suppressive subtractive hybridization analysis. Fed Eur Biochem Soc 576:320–324.

Uyeda K, Yamashita H, Kawaguchi T. 2002. Carbohydrate responsive element-binding protein (ChREBP): A key regulator of glucose metabolism and fat storage. Biochem Pharmacol 63:2075–2080.

Villanueva CJ, Monetti M, Shih M, Zhou P, Watkins SM, Bhanot S, Farese RV Jr. 2009. Specific role for acyl CoA:Diacylglycerol acyltransferase 1 (Dgat1) in hepatic steatosis due to exogenous fatty acids. Hepatology 50:434–442.

Wahli W, Devchand PR, A IJ, Desvergne B. 1999. Fatty acids, eicosanoids, and hypolipidemic agents regulate gene expression through direct binding to peroxisome proliferator-activated receptors. Adv Exp Med Biol 447:199–209.

Wang GL, Fu YC, Xu WC, Feng YQ, Fang SR, Zhou XH. 2009. Resveratrol inhibits the expression of SREBP1 in cell model of steatosis via Sirt1-FOXO1 signaling pathway. Biochem Biophys Res Commun 380:644–649.